Evaluation of Seasonal Forecasts for the Fire Season in Interior Alaska

AKILA SAMPATH,[a] UMA S. BHATT,[a] PETER A. BIENIEK,[b] ROBERT ZIEL,[c] ALISON YORK,[c] HEIDI STRADER,[d] SHARON ALDEN,[d] RICHARD THOMAN,[e] BRIAN BRETTSCHNEIDER,[f] EUGENE PETRESCU,[f] PEITAO PENG,[g] AND SARAH MITCHELL[a]

[a] *Department of Atmospheric Sciences, Geophysical Institute, University of Alaska Fairbanks, Fairbanks, Alaska*
[b] *International Arctic Research Center, University of Alaska Fairbanks, Fairbanks, Alaska*
[c] *Alaska Fire Science Consortium, International Arctic Research Center, University of Alaska Fairbanks, Fairbanks, Alaska*
[d] *Predictive Services, Alaska Interagency Coordination Center, Alaska Fire Service, Fort Wainwright, Alaska*
[e] *Alaska Center for Climate Assessment and Policy, International Arctic Research Center, University of Alaska Fairbanks, Fairbanks, Alaska*
[f] *NOAA/National Weather Service Alaska Region, Anchorage, Alaska*
[g] *Climate Prediction Center, NOAA/NWS/NCEP, College Park, Maryland*

(Manuscript received 1 November 2019, in final form 16 December 2020)

ABSTRACT: In this study, seasonal forecasts from the National Centers for Environmental Prediction (NCEP) Climate Forecast System, version 2 (CFSv2), are compared with station observations to assess their usefulness in producing accurate buildup index (BUI) forecasts for the fire season in Interior Alaska. These comparisons indicate that the CFSv2 June–July–August (JJA) climatology (1994–2017) produces negatively biased BUI forecasts because of negative temperature and positive precipitation biases. With quantile mapping (QM) correction, the temperature and precipitation forecasts better match the observations. The long-term JJA mean BUI improves from 12 to 42 when computed using the QM-corrected forecasts. Further postprocessing of the QM-corrected BUI forecasts using the quartile classification method shows anomalously high values for the 2004 fire season, which was the worst on record in terms of the area burned by wildfires. These results suggest that the QM-corrected CFSv2 forecasts can be used to predict extreme fire events. An assessment of the classified BUI ensemble members at the subseasonal scale shows that persistently occurring BUI forecasts exceeding 150 in the cumulative drought season can be used as an indicator that extreme fire events will occur during the upcoming season. This study demonstrates the ability of QM-corrected CFSv2 forecasts to predict the potential fire season in advance. This information could, therefore, assist fire managers in resource allocation and disaster response preparedness.

KEYWORDS: Ensembles; Hindcasts; Seasonal forecasting; Climate models; Model evaluation/performance; Reanalysis data

1. Introduction

Wildfires are a natural component of boreal forest ecological processes (Rowe and Scotter 1973; Bond-Lamberty et al. 2007). As Alaska continues to warm, the frequency and areal extent of wildfires are increasing, as is the demand for firefighting resources (Chapin et al. 2008). Interior Alaska is dominated by 60%–70% boreal forest coverage (Nowacki et al. 2003) and is home to approximately 100 000 inhabitants. Most of this population lives in remote villages where access through conventional transportation options is limited. Thus, the most common way to mitigate fires that threaten rural indigenous communities is via expensive air tankers (Todd and Jewkes 2006).

Weather is the most important factor influencing fire behavior. Regions with warm and dry atmospheric conditions have more frequent and more severe fire events (Flannigan et al. 2009; Partain et al. 2016). In Alaska, the seasonal severity of boreal forest fires changes frequently based on the forest floor fuel loads and their flammability. Dollard (2020) distinguished the fire season into four subseasons to capture the fire behavior based on the primary fire drivers: the wind-driven season (1 April–10 June), the duff-driven season (11 June–9 July), the cumulative drought season (10 July–15 August), and the diurnal effect-driven season (16 August–30 September). In each subseason, fuel availability and weather conditions affect fire growth differently. For example, frontal winds contribute to fire growth during the wind-driven season, whereas in the duff-driven season, longer days combined with warm and dry conditions result in the production of fuel loads from dried tundra and spruce vegetation, which in turn supports intense fires. The cumulative drought season is dominated by severe and frequent fires, as below-normal precipitation and high air temperatures contribute to dry fuel loads. Eventually, the fire season subsides during the diurnal effect season, when shorter, cooler days limit the occurrence of fires.

Information about the availability of dry fuel loads on the forest floor and the local weather conditions in each subseason is

Supplemental information related to this paper is available at the Journals Online website: https://doi.org/10.1175/WAF-D-19-0225.s1.

Corresponding author: Akila Sampath, asampath@alaska.edu

Publisher's Note: This article was revised on 20 July 2021 to add additional authors and update the Acknowledgments section, and again on 3 August 2021 for an additional edit to the Acknowledgments section.

DOI: 10.1175/WAF-D-19-0225.1

necessary for fire managers to evaluate the growth and severity of fires in boreal forests. The Canadian forest fire weather index system (FWI; Van Wagner 1987) is commonly used to connect boreal fire behavior to local weather conditions (Horel et al. 2014). In the FWI system, the buildup index (BUI) is a unitless quantity that estimates the total amount of dry forest fuel available for combustion and helps identify areas with increased fire potential. Alaskan fire managers assess fire severity and develop effective preventive action plans based on the BUI (Partain et al. 2016). According to Arpaci et al. (2013), the BUI has been identified as the best indicator of the severity of seasonal fires and overall flammability of boreal forest fires. Climate–fire relationships are location specific (Littell et al. 2009); thus, fire managers consider the evaluation of the BUI in predictive service areas (PSAs) to be ideal for fire-fighting logistics because PSAs encompass regions with unique weather conditions.

Studies have demonstrated the applicability of NCEP's operational forecast system, the Climate Forecast System, version 2 (CFSv2), for hydrological and soil moisture predictions (Yuan et al. 2011; Mo et al. 2012). The present study aims to assess the usefulness of the CFSv2 temperature, precipitation, and specific humidity forecasts that are available in early March for producing BUI forecasts in each PSA for the Interior Alaska fire season. Application of CFSv2 forecasts in BUI prediction requires a preprocessing step to minimize the forecast biases, which hinder the better representation of local weather. For this purpose, this study also focuses on correcting the forecast biases using the quantile mapping (QM) method. The QM technique is most commonly used in climate change applications; however, this study explores its usage for seasonal prediction purposes. The proposed correction procedures are developed based on the discussions present in Cannon et al. (2015). The CFSv2 precipitation and temperature forecasts are important to calculate BUI and are corrected to ensure no additional artifacts are added to the forecasts. This step retains the original distributions of the ensemble forecasts, thus maximizing their applicability to seasonal extreme weather prediction applications. After the correction, the performance of the forecasts is investigated by comparing the temperature, precipitation, and BUI forecasts with station observations at the PSA scale. Overall, the usefulness of the corrected CFSv2 ensemble forecasts in determining the potential predictability of BUI forecasts is demonstrated.

This paper is organized as follows: section 2 explains how the QM correction method is applied to the CFSv2 ensemble forecasts, including a description of the model forecasts, observations, and statistical analysis. Section 3 presents the CFSv2 forecast evaluations, the corrected CFSv2 forecasts, the skill analysis of the corrected forecasts, and a discussion of their ability to predict the BUI. Section 4 provides conclusions and recommendations based on the results of the QM-corrected forecasts.

2. Data

a. *Predictive service area station observations*

Fire managers use daily BUI values that are calculated from in situ observations and are specific to each PSA (Fig. 1) in their early preparation plans. These observations are archived and available to fire professionals in the United States via the MesoWest web interface, and are widely used for evaluating model forecasts in fire weather applications (Horel et al. 2014). Data resources from the Alaska Fire and Fuels (AKFF; https://akff.mesowest.org/) include both the National Weather Service (NWS) station and the Remote Automated Weather System (RAWS; Horel and Dong 2010) networks.

All station observation data in each PSA (Fig. 1, black circles) are averaged together to calculate the daily PSA data. In this study, observational data from each PSA are used to develop PSA-specific correction procedures over the period of 1994–2010 and to evaluate the CFSv2 from 1994 to 2017. The Fairbanks–Tanana Valley region, which has a continental climate, is an area of focus for fire managers in Interior Alaska (McCorkle et al. 2018). The Tanana Valley West PSA has the highest density of observations (Fig. 1). Therefore, only the analysis for this PSA is presented and discussed in the main body of the paper.

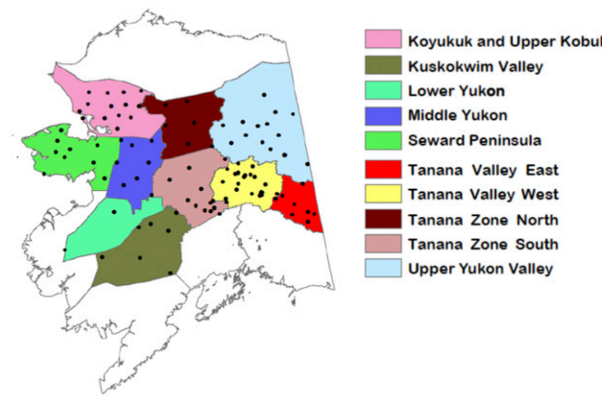

FIG. 1. Fire predictive service area (PSA) divisions. The legend labels show the 10 Interior Alaska PSA names that are analyzed in this study. MesoWest stations are shown by the black circles. See text for further details.

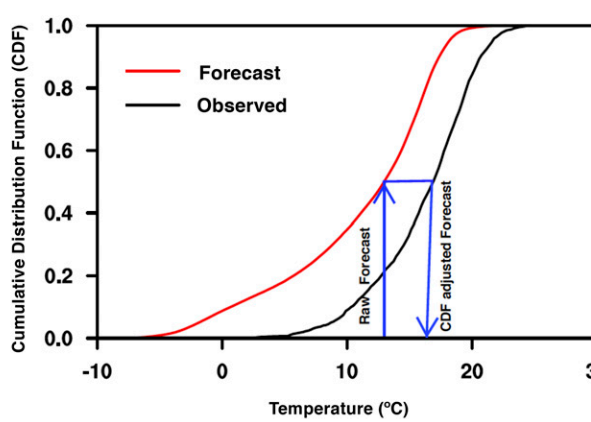

FIG. 2. Schematic view of the quantile mapping (QM) correction method for a temperature forecast for the Tanana Valley West. QM for precipitation looks similar.

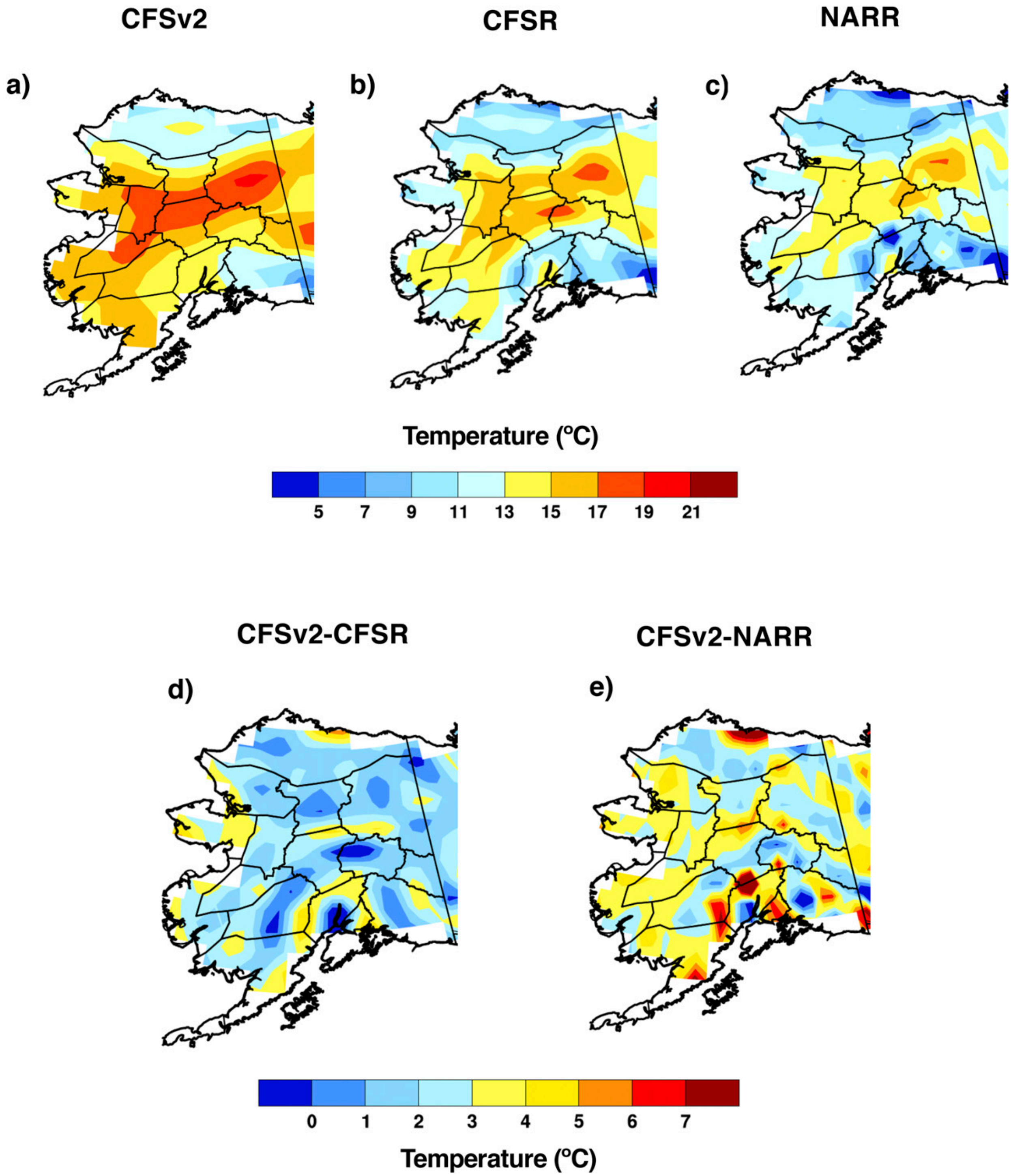

FIG. 3. JJA temperature (°C) for the period of 1982–2010: (a) climatology of CFSv2, (b) climatology of CFSR, (c) climatology of NARR, (d) CFSv2 minus CFSR, and (e) CFSv2 minus NARR.

b. Climate Forecast System Reanalysis

The NCEP Climate Forecast System Reanalysis (CFSR; 1982–2010) is a high-resolution reanalysis product that includes coupled atmosphere, ocean, land surface, and sea ice climate model components (Saha et al. 2010). This integrates a spectral atmospheric model (Saha et al. 2006) at a horizontal resolution of ~38 km (T382), with 64 hybrid vertical levels. In addition to a full range of observations, satellite radiances are assimilated in this reanalysis.

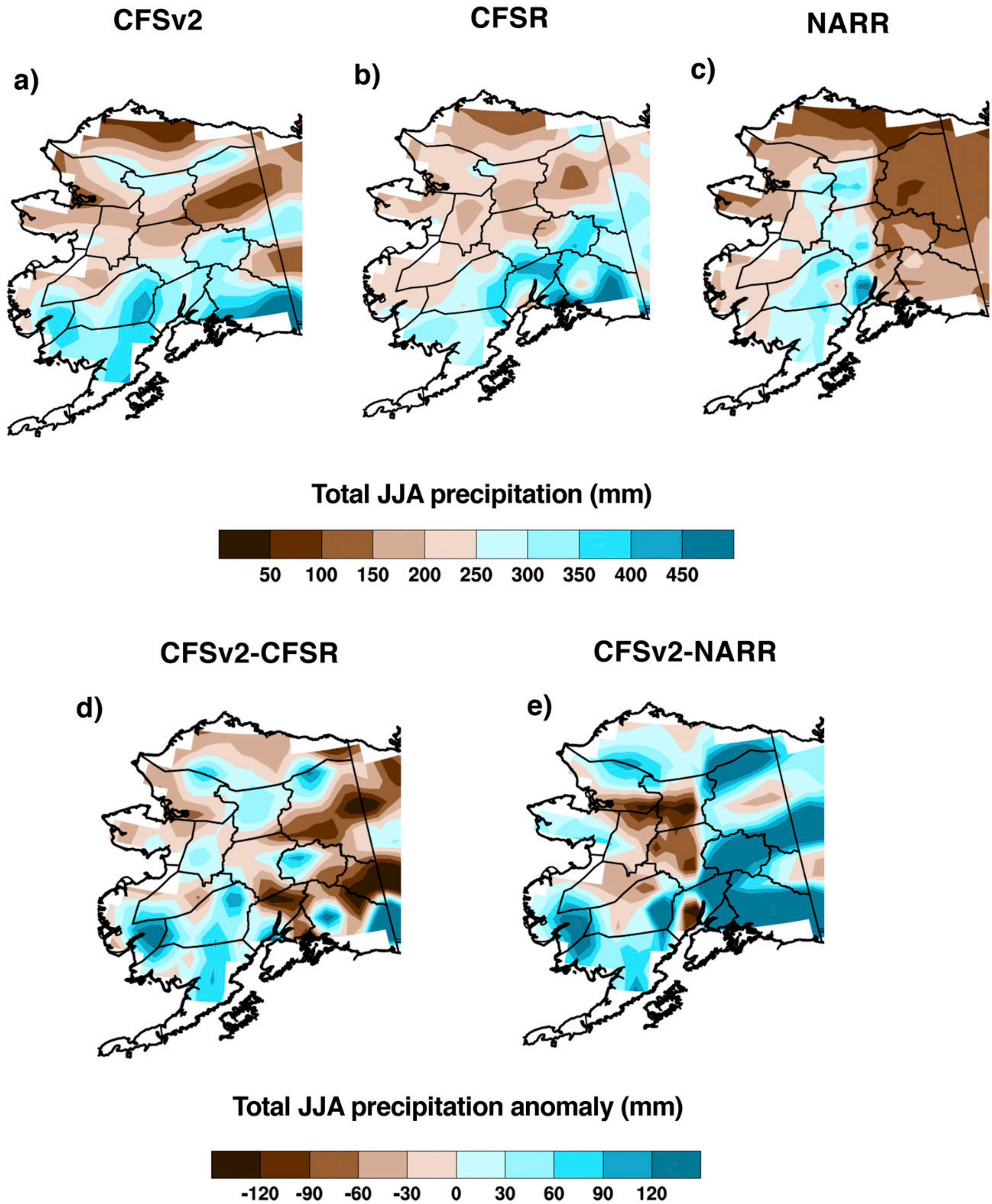

FIG. 4. As in Fig. 3, but for JJA precipitation (mm).

c. North American Regional Reanalysis

The NCEP North American Regional Reanalysis (NARR; 1979–present) is a dynamically consistent, high-resolution model with substantially improved atmospheric circulation throughout the troposphere (Mesinger et al. 2006). This reanalysis is generated using the high-spatial-resolution NCEP Eta model with a horizontal resolution of 32 km and 45 vertical

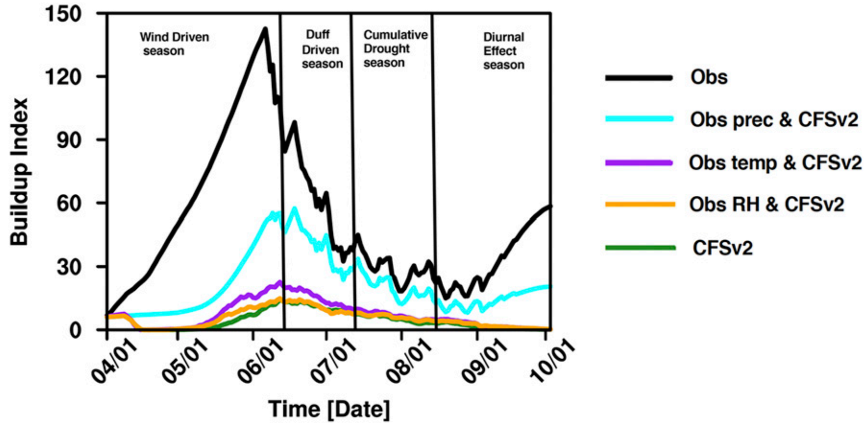

FIG. 5. BUIs for the Tanana Valley West (1994–2017) PSA are calculated using observations only (black), model with observed precipitation (cyan), model with observed temperature (purple), model with observed relative humidity (orange), and model only (green).

layers. The Regional Data Assimilation System (RDAS) is integrated with this reanalysis. The NARR includes accurately assimilated precipitation (Becker et al. 2009) and 2-m temperature fields that have been shown to be in agreement with observations (Mesinger et al. 2006). This reanalysis also includes a full range of observations.

d. CFSv2 forecast

The NCEP CFSv2 system is a coupled operational ensemble forecast system that consists of atmosphere, ocean, land, and sea ice models (Saha et al. 2014). The CFSv2 spectral atmospheric component model is the Global Forecast System (GFS), which is run at a T126 (~100 km) horizontal resolution with 64 vertical sigma-pressure hybrid levels.

CFSv2 hindcasts (1982–2010) have 24 ensemble members and are initialized using CFSR data. CFSv2 real-time forecasts (2011–present) have 120 ensemble members (Becker and Van Den Dool 2016). These CFSv2 forecasts use initial conditions from the seasonal Climate Data Assimilation System, version 2. The hindcasts and forecasts are both initialized every 5 days at four coordinated universal time (UTC) cycles (0000, 0600, 1200, and 1800).

3. Methods

a. The buildup index

The BUI calculation uses a set of nonlinear mathematical formulations that require data on the daily total precipitation, 2-m temperature, and relative humidity at local solar noon (Van Wagner 1987). The relative humidity is calculated using the forecasted CFSv2 temperature and specific humidity. Solar noon is approximately 1400 AKST in the eastern Interior Alaska region (i.e., close to the Canadian border) and 1500 AKST in the western Interior Alaska region (i.e., adjacent to the Bering Sea). Due to the wide range of local noon times, 0000 UTC (1500 AKST) CFSv2 forecast values are used in the BUI calculations. Therefore, in this study, it is assumed that the uncertainty due to the differences between the values at local noon in the forecast and those in the PSA is marginal and does not contribute to any major biases. The total daily precipitation is computed by summing the precipitation from all four cycles (0000, 0600, 1200, and 1800). The BUIs are then calculated for each PSA from the daily weighted average of the CFSv2 temperature and precipitation forecasts. These values are later evaluated by comparing them with the BUI values calculated from the PSA observations to explore the sensitivity of the BUI to weather parameters. In this study, BUIs are calculated using the FORTRAN 95 version of the FWI source code (Wang et al. 2015).

b. Quantile mapping

Downscaled forecasts have been created using QM, and these forecasts are reasonably comparable to observations (Wood et al. 2004). In this study, the nonparametric empirical QM method (i.e., Zhao et al. 2017) is used to correct the CFSv2 seasonal forecast biases. The QM correction method is implemented for temperature and precipitation variables for the calibration period of 1994–2010 and validated for the period of 1994–2017. In the QM correction method, the cumulative distribution function (CDF) of the forecast variables is shifted toward those of the observations. Therefore, each quantile of the model data is mapped to the corresponding quantile in the observations (Zhao et al. 2017).

To correct the data, daily area-weighted averages of the forecasted temperature and precipitation are first calculated for each PSA. Then, the time series of both the forecasts and the corresponding PSA observations are smoothed using a 31-day moving average window (e.g., Pierce et al. 2015). The 31-day moving window ensures that noise and extreme values are removed from the observations before the data are corrected using the QM correction method. In addition, this smoothing process facilitates the comparison of time series observations with time series weighted-area averages of gridded data. The smoothing process is repeated with various window lengths to explore the sensitivity of the observational data to smoothing processes. Overall, the 31-day window has been determined to best capture the seasonal observations.

Next, lookup tables are created for each PSA, with empirical quantiles of the forecast values and empirical quantiles of the observations using the CDF (Fig. 2). An inverse CDF value for the daily uncorrected forecast (or corrected forecast) is produced by looking up the quantile corresponding to the closest forecast value in the forecast calibration set (i.e., 1994–2010). This forecasted quantile value is then matched to the observed quantile value to determine the associated observed value [Eq. (1); see Fig. 2]:

$$x_{\text{corr-fcst}}(t) = F_{\text{obs}}^{-1}\{F_{\text{fcst}}[x_{\text{fcst}}(t)]\}, \tag{1}$$

$$x_{\text{corr-temp-fcst}}(t) = \frac{x_{\text{fcst}}(t) + F_{\text{obs}}^{-1}\{F_{\text{fcst}}[x_{\text{fcst}}(t)]\}}{2}, \tag{2}$$

$$x_{\text{corr-prec-fcst}}(t) = \frac{r^{-1}x_{\text{fcst}}(t) + F_{\text{obs}}^{-1}\{F_{\text{fcst}}[x_{\text{fcst}}(t)]\}}{2}. \tag{3}$$

Here, F_{fcst} is the CDF of the uncorrected forecast x_{fcst}, and F_{obs}^{-1} is the inverse CDF of the observations x_{obs} at time t. The corrected forecast at time t for the forecast that best matches observations is defined as $x_{\text{corr-fcst}}$ [Eq. (1)]. The corrected temperature and precipitation forecasts beyond the observations are defined as $x_{\text{corr-temp-fcst}}$ [Eq. (2)] and $x_{\text{corr-prec-fcst}}$ [Eq. (3)], respectively. The precipitation values are rescaled to reduce the peak values using a scaling factor r. Here, r is the ratio of the average of all values in the calibration set of observations to the average of all values in the uncorrected forecast. Incorporating scaling processes into correction procedures has been shown to result in better corrected precipitation forecasts (Cannon et al. 2015). In this study, the proposed correction methods are intended to correct any major biases associated with the shape and magnitude of the ensemble members at the daily time scale but not to correct the original model physics of the forecasts (for a discussion on correcting for model physics, see Bürger et al. 2011).

c. Skill assessment of the CFSv2 forecast

The CFSR and NARR are used to evaluate the CFSv2 temperature and precipitation data from 1982 to 2010. The datasets, variables, and postprocessing methods are described in a flowchart (see the appendix).

The PSA area-weighted averages of the corrected and uncorrected forecast temperature and precipitation are used for the June–July–August (JJA) skill assessment for individual ensemble members with respect to the PSA observations spanning 1994–2017. The skill of the corrected forecast ensemble members at the daily time scale is assessed for all 10 PSAs using root-mean-square error (RMSE) and skill score (SS) values (Wilks 2006). The SS, defined as a percentage, is determined for the individual forecast ensemble members [Eq. (4)]:

$$\text{skill score (SS)} = \frac{\text{RMSE}_{\text{uncorr}} - \text{RMSE}_{\text{corr}}}{\text{RMSE}_{\text{uncorr}}} \times 100\%. \tag{4}$$

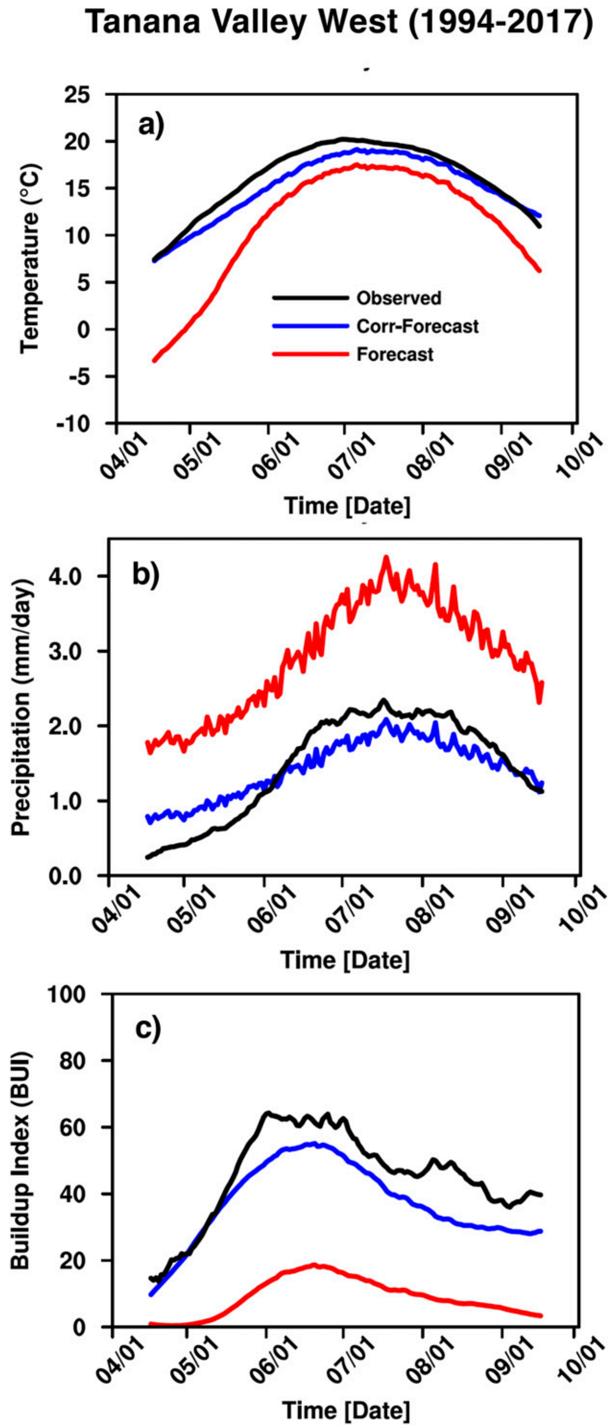

FIG. 6. Daily mean seasonal cycle over 1994–2017 for the Tanana Valley West: (a) temperature, (b) precipitation, and (c) BUI.

In Eq. (4), $\text{RMSE}_{\text{uncorr}}$ represents the RMSE of the uncorrected forecasts, and $\text{RMSE}_{\text{corr}}$ is the RMSE of the corrected forecasts. A high SS indicates high forecasting skill.

A quantile classification (Freund and Perles 1987; Hyndman and Fan 1996) is used to further postprocess the corrected BUI

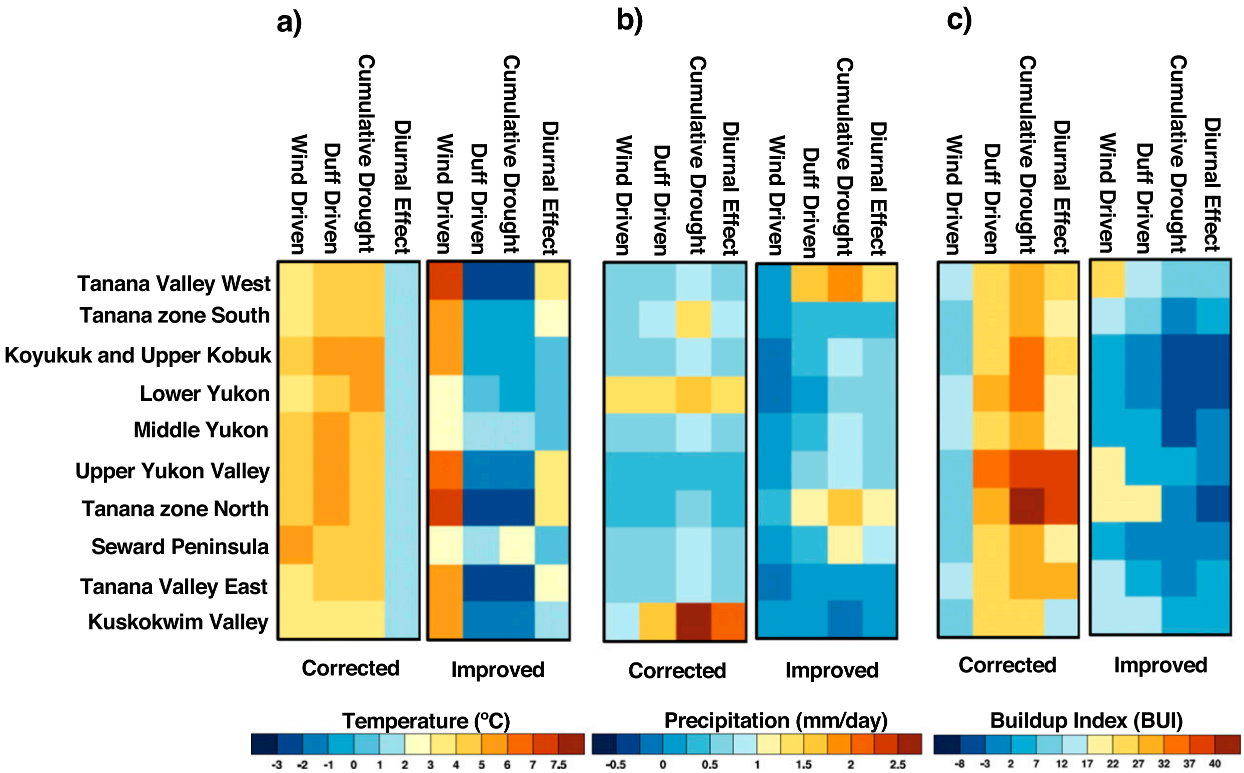

FIG. 7. Corrected and improved RMSEs (1994–2017) for (a) temperature, (b) precipitation, and (c) BUI over all 10 Interior Alaska PSAs at the four subseasonal scales. The improved RMSE is uncorrected minus corrected.

forecasts. The corrected BUI ensemble members are grouped into five equal-sized bins based on their statistical rank: zeroth quantile (minimum), first quantile (Q1), second quantile (Q2), third quantile (Q3), and fourth quantile (Q4). In this study, the fourth quantile is used to describe the predictability of QM-corrected BUI forecasts at the subseasonal scale for each PSA.

4. Results and discussion

a. *Climatology of the temperature and precipitation forecasts*

The uncorrected JJA CFSv2 ensemble forecast data are assessed for their prediction skill with respect to the CFSR and NARR data over Interior Alaska (Figs. 3 and 4). The spatial distributions of the long-term means show that temperatures vary from 13° to 19°C for CFSv2 and that they capture the range found in the CFSR and NARR data across Interior Alaska (Figs. 3a–c). The temperature differences between CFSv2 and CFSR range from 1° to 3°C (Fig. 3d) and from 2° to 5°C between CFSv2 and NARR (Fig. 3e), which demonstrates a warm bias in the CFSv2 forecasts across Interior Alaska (relative to NARR).

The CFSv2 JJA total precipitation patterns are comparable to those of CFSR and NARR (Figs. 4a–c). In most of the low-precipitation regions, the accumulated JJA CFSv2 precipitation forecasts are approximately 30 mm lower than those of CFSR and NARR (Fig. 4c). The warm and dry weather patterns in the CFSv2 forecasts are in better agreement with CFSR than with NARR. These findings suggest that CFSv2 forecasts are reasonably comparable to the CFSR and NARR datasets and are reliable for the Interior Alaska region. However, the warm and dry weather patterns in the CFSv2 forecasts are in better agreement with CFSR than with NARR.

b. *Bias correction and its impacts*

To explore the relationship between the calculated BUIs and the local fire weather conditions, sensitivity tests were performed using the daily weighted time series of observations and CFSv2 forecasts for the Tanana Valley West PSA (Fig. 5). The following combinations of BUI-affecting parameters are tested: 1) forecasted temperature and relative humidity (RH) with observed precipitation, 2) forecasted precipitation and RH with observed temperature, and 3) forecasted temperature and precipitation with observed RH.

The results from the sensitivity test show that precipitation affects the BUI more than the rest of the included meteorological variables, followed by temperature (Fig. 5). The sensitivity of the BUI to precipitation confirms that fire weather indices are particularly sensitive to seasonal precipitation (Horel et al. 2014). In the cumulative drought season, the combination of observed precipitation with forecasted temperature and RH best captures the BUI calculated from the station observation data. Based on the results of the sensitivity tests, this study proposes to correct the daily CFSv2 precipitation and temperature fields using the QM correction method to match the observations at the climatological scale (Fig. 6). Although RH is not corrected using the QM correction method, the corrected temperature is used to calculate RH from the CFSv2-specific humidity to preserve the thermodynamic consistency between RH and temperature.

Comparing the time series between the CFSv2 forecasts and observational data shows a cold bias in the 2-m temperature forecasts and a wet bias in the precipitation forecasts for the Tanana Valley West PSA (Fig. 6). After the QM correction, the cold bias in early spring is reduced and matches the observation values (approximately 7°–12°C) well (Fig. 6a). This correction also removes the aforementioned precipitation bias, which is two times larger than the observed values, but it does not remove the observed precipitation biases in the wind-driven season (Fig. 6b). Overall, this correction procedure improves the JJA long-term mean temperature value from 15.5° to 17.5°C and improves that of precipitation from 3.4 to 1.6 mm day^{-1}. The corrected temperature and precipitation change the long-term mean JJA BUI value from 12 to 42 (Fig. 6c), which is reasonably close to the observed BUI of 52. The forecasts for the other nine Interior Alaska PSAs are similarly improved after applying the QM correction method (see Figs. S1–S3 in the online supplemental material). These findings indicate that this correction process is key for improving forecasts at the climatological scale with reference to observations.

The RMSEs of the corrected temperature forecasts range from 3° to 6°C for all PSAs in all but the diurnal effect season, when the individual PSA RMSEs range from 1° to 2°C (left panel of Fig. 7a). This means that the applied QM correction method reduces the temperature RMSE by approximately half. The corrected precipitation forecast RMSEs range from 0 to 2.5 mm day^{-1}, and the improvements range from −0.25 to 2 mm day^{-1} for all subseasons (Fig. 7b). Overall, the corrected precipitation error is reduced by approximately 25%. The corrected temperature and precipitation forecasts improve the RMSE values of the BUI forecasts for all PSAs (Fig. 7c). The corrected BUI RMSEs range from 7 to 45. Improvements in the BUI range in magnitude from −8 to 27. The proposed correction methods do have limitations with regard to correcting extreme conditions in precipitation and temperature forecasts, which introduces forecast errors. The skill of the temperature forecasts also decreases with the addition of a "new extreme" whenever the actual forecast values are close to the observed values (e.g., Wilks and Hamill 2007). Therefore, the correction methods cannot mitigate the prediction errors associated with extreme conditions of several ensemble members.

The SS assesses the degree to which the corrected ensemble forecasts are more skillful than the uncorrected forecasts (Fig. 8). A corrected forecast with a skill equal to that of the uncorrected forecast would have an SS of 0%, and a corrected forecast that is more skillful than the uncorrected forecast would have a positive SS value. The SSs of the corrected BUI forecasts for most of the PSAs show an approximately 30% improvement (Fig. 8). The skill analysis also suggests that ensemble forecasts can be useful in identifying rare events, as shown for the 2004, 2005, and 2015 fire seasons, which resulted

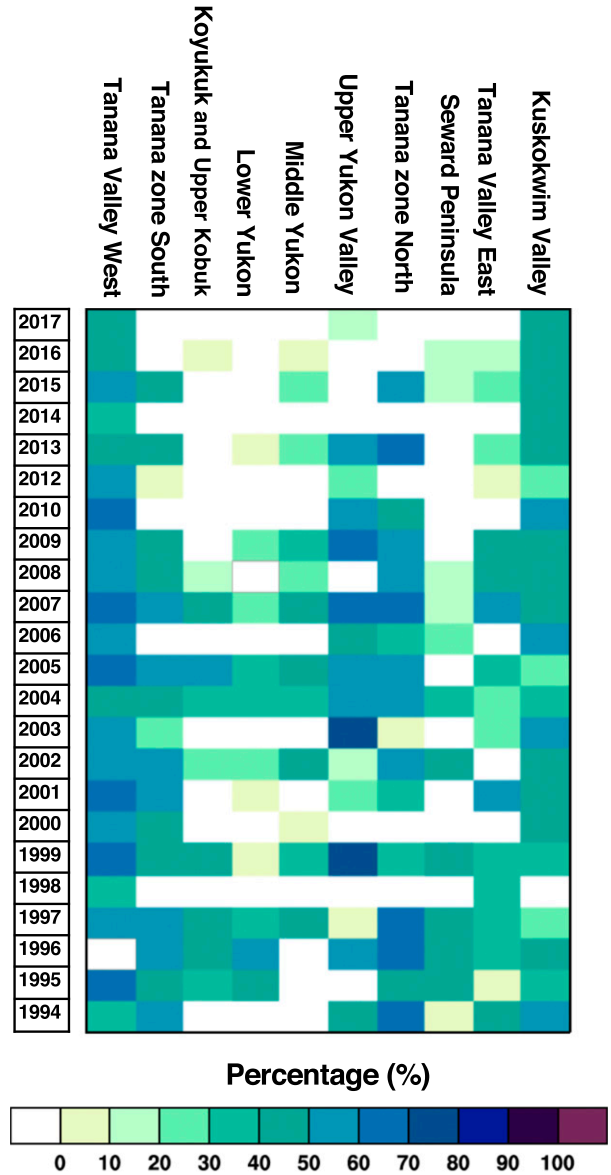

FIG. 8. Skill score of JJA corrected forecasts BUI over the 10 PSAs. The 100% percentage indicates perfect forecasts, and 0% percentage indicates random forecasts.

in SS values greater than or equal to 40%. During these years, the calculated burn areas for some of the PSAs are larger than those in other years. These findings suggest that the corrected CFSv2 forecasts have the ability to predict the observed large fire years.

c. Case studies: The record fire years 2004, 2005, and 2015

The 2004, 2005, and 2015 fire seasons are considered to be the worst in Alaska's 56-yr record in terms of area/acres burned (4 million acres or more) (Partain et al. 2016). Further analyses and discussions regarding these fire seasons are based on their impacts in the Tanana Valley West PSA, which is the PSA that is most representative of the Interior Alaska climate.

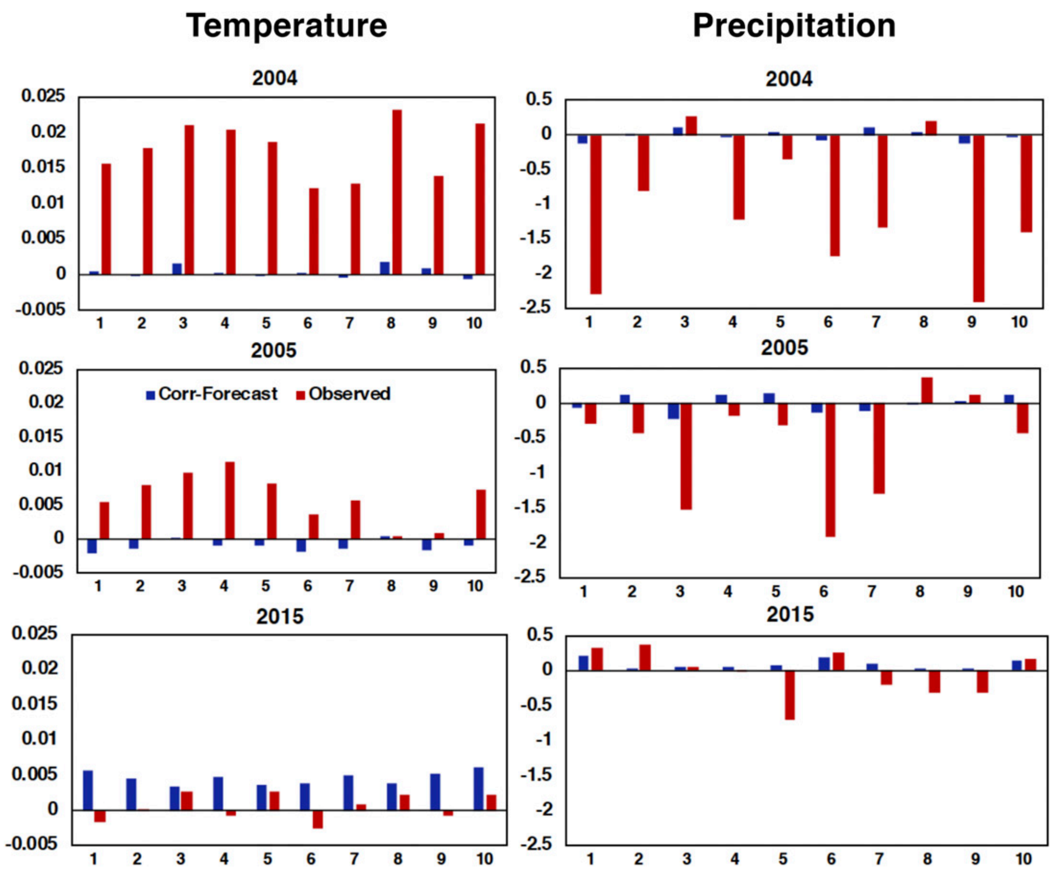

FIG. 9. Standardized anomaly patterns of JJA (left) temperature and (right) precipitation for the high fire activity seasons of 2004, 2005, and 2015. The 10 Interior Alaska PSAs, numbered from 1 to 10, are Tanana Valley West, Tanana zone South, Koyukuk and Upper Kobuk, Lower Yukon, Middle Yukon, Upper Yukon Valley, Tanana zone North, Seward Peninsula, Tanana Valley East, and Kuskokwim Valley, respectively.

This study assesses the corrected forecast skill for large fire years in Interior Alaska using normalized anomaly indices. The anomalies are normalized by dividing the anomaly by the standard deviation. Temperature and precipitation anomalies are determined for the years 2004, 2005, and 2015 for both the corrected forecasts and the observations, taking the 1994–2017 JJA forecast means as the climate normal. The above-normal temperature anomalies (+0.015 or higher) and below-normal precipitation anomalies (−1.5 or higher) suggest that the forecasts show larger variability for 2004, the year during which the largest area was burned, than for other years (Fig. 9). The forecast anomalies from 2015 have a much lower variability than those in other years because of the larger number of ensemble members, i.e., 120; in 2004 and 2005, there were only 24 ensemble members. The temperature and precipitation anomalies from 2015 suggest that forecasts with more ensemble members have better prediction skills, as they were predicted better than those from 2004 to 2005 (Fig. 9; Becker et al. 2013). Notably, the forecasts could better capture anomalies and extremes than the observational network. This is attributed to the fact that the forecast anomalies are calculated for every grid cell, while the PSA observation anomalies are based on relatively few, sparse point measurements.

The comparison of the JJA ensemble means to the observations for the large fire seasons suggests that the ensemble means of both the temperature and precipitation forecasts roughly capture the variable observations for the duff-driven season and cumulative drought seasons (Fig. 10). Consistent with the 2015 anomaly results (Fig. 9), the 2015 ensemble mean forecasts predict observations better than the 2004 and 2005 forecasts. However, the ensemble mean forecasts for temperature, precipitation, and BUI fail to capture the observed JJA peak conditions and underestimate the observed BUI. This suggests that the BUI ensemble mean values may not be useful in predicting the BUI values that correspond to extreme fire weather conditions. The ensemble spread of the BUI is large enough to capture the extremes of the observed BUI on any given day. These findings suggest that the classification of the BUI ensemble members can preserve the fire seasonality corresponding to the observed BUI values and can be useful in predicting severe fire events. Furthermore, considering individual ensemble members and their uncertainties could be

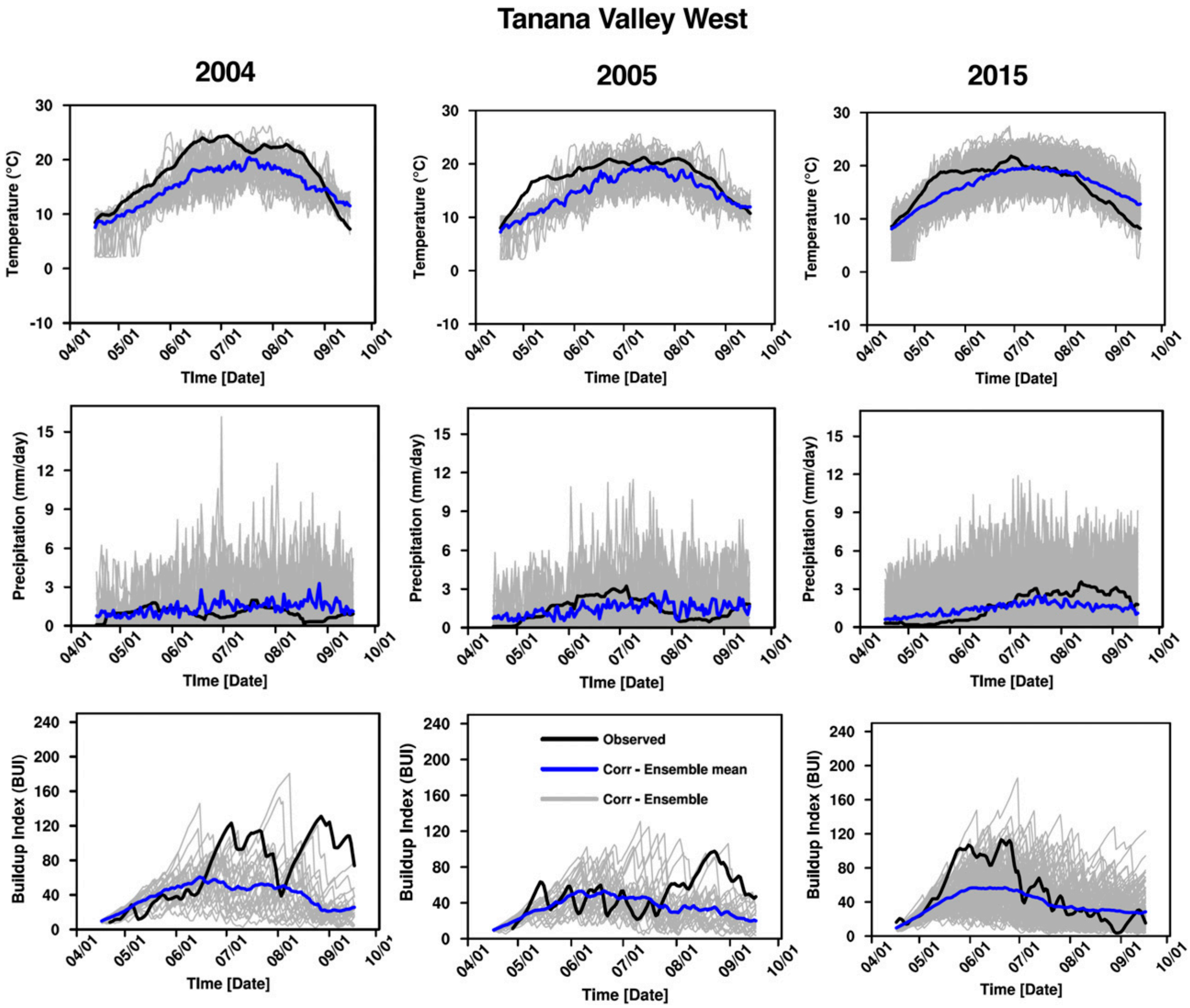

FIG. 10. Daily mean seasonal cycle of Tanana Valley West temperature, precipitation, and BUI for 2004, 2005, and 2015, respectively.

useful for determining the predictability of the CFSv2 forecast. The observed BUI analysis (Fig. 10; dark line) shows that forecasts of high temperatures precede peak BUIs by approximately two weeks. This indicates that peak temperatures and high-BUI events within a two-week window should be simultaneously considered for fire action planning in Interior Alaska PSAs. Furthermore, a study by Arpaci et al. (2013) reported better performance of both the daily temperature and the BUI in predicting extreme fire years.

d. Discussion of BUI predictability

Based on the work presented above, it would be useful to ensure the practicability of the QM-corrected BUI forecasts in predicting extreme fire events in the duff-driven and cumulative drought seasons. For this purpose, the ensemble members are ranked based on their corresponding quantiles (Fig. 11). The forecasted BUI values in the Q4 set closely match the observed peak BUI values in the duff-driven and cumulative drought seasons (Fig. 11). For 2004, the anomalous maximum BUI value is forecasted in the cumulative drought season, in which the Q4 BUI increases as the observation value decreases. The skill of the temperature and precipitation forecasts may contribute to these anomalous Q4 BUI values that contradict the observed BUI in the cumulative drought season. This observed minimum Q4 BUI forecast may arise due to terrain elevation differences between the forecast model, which uses grid-averaged elevations, and point-based observations. Therefore, Q4 BUI forecasts have the potential to predict the dry fuel loads and weather conditions associated with extreme fire seasons. Moreover, the anomalous Q4 BUI forecasts can be used as an indicator of extreme fire events in the upcoming season.

The source of forecast predictability can be determined using a so-called persistence measurement. Typically, in a persistence measurement, future forecasts are assumed to maintain the current observed anomaly conditions (Spillman and Alves 2009). In this case, minimum-skill BUI forecast values of 150 or higher in the cumulative drought season would be repeated in the future forecast for the same season. If such

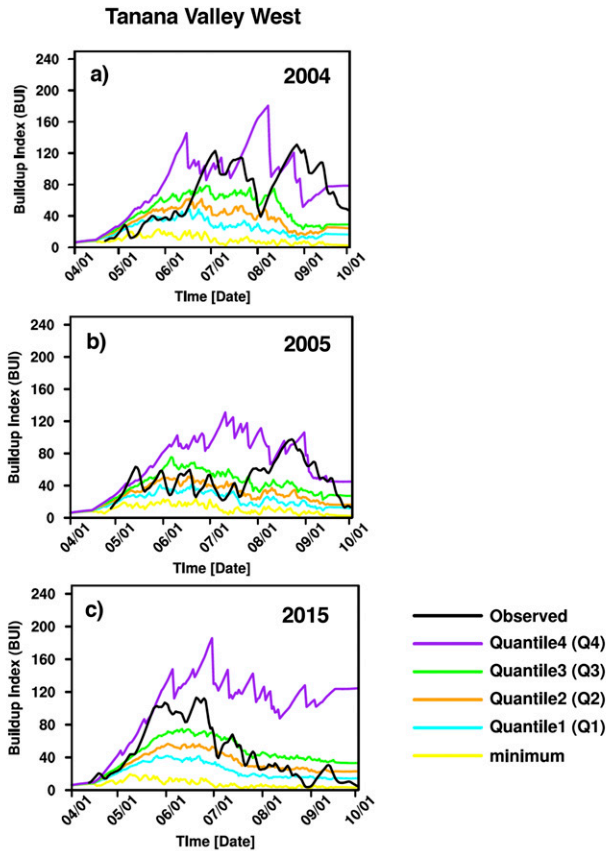

FIG. 11. Tanana Valley West quantile-based BUI for (a) 2004, (b) 2005, and (c) 2015. Results are similar for other PSAs.

persistence is identified in the forecast, the fire season is labeled an extreme fire year in which extreme fire events are likely to occur. These anomalous forecast conditions are observed in the duff-driven and cumulative drought seasons in the worst fire years.

The prediction skill of the JJA Q4 BUI is assessed by comparing the observed total acres burned and the observed BUI from 1994 to 2017 for all PSAs (Fig. 12). Extreme changes in the BUI are found in both 2004 and 2009. Similarly, the Q4 BUI exceed the threshold value of 150 in the cumulative drought season. These findings support the usefulness of persistence forecasts for identifying seasons with severe fire events (Fig. 11). Overall, these results are consistent across all PSAs, indicating that CFSv2 forecasts can provide decision-makers with valuable information on the maximum probable value of the BUI corresponding to an extreme fire season.

5. Summary and conclusions

Seasonal fire forecasting is a challenging problem for climate scientists. This study investigates the seasonal predictions of 1–3-month leads using the CFSv2 March forecasts for JJA using all available ensembles for 1994–2017. The spatial comparison of JJA CFSv2 climatology forecasts (Figs. 3 and 4) with the CFSR and NARR data shows a positive 2-m temperature bias of approximately 2°C and a negative precipitation bias of approximately 30 mm in CFSv2 over Interior Alaska.

Given the lack of gridded observational data for Interior Alaska, correction procedures are developed using observational time series data for temperature, precipitation, and relative humidity, all of which are commonly used by fire managers in decision-making procedures. The nonparametric QM correction method is applied to correct the time series of the CFSv2 temperature and precipitation forecasts because it 1) simplifies the correction procedure and 2) keeps the distribution of the actual ensemble forecasts without introducing uncertainty into the forecast physics. In this method, the shape and spread of the ensemble forecasts are kept similar to that of the original forecast, which makes them useful for predicting extreme weather events.

Evaluations of seasonal QM-corrected forecasts of temperature, precipitation, and BUIs are performed for all PSAs. This evaluation shows that the QM correction method removes a portion of the temperature and precipitation biases associated with forecast errors. Furthermore, these corrections show an improvement in the BUI forecasts, which is reflected in the calculated JJA mean BUI increasing from 12 to 42 based on the corrected JJA mean temperature and precipitation forecasts of 17.5°C and 1.6 mm day^{-1}, respectively. Thus, these findings demonstrate that QM-corrected CFSv2 ensemble forecasts are able to capture the seasonal-scale features of

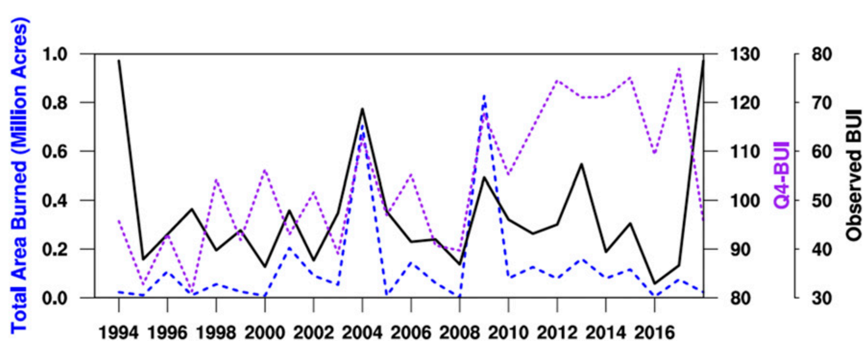

FIG. 12. Tanana Valley West observed JJA total acreage burned (blue dashed line), forecasted Q4 BUI (purple dotted line), and observed BUI (black line). Plots for other PSAs look similar.

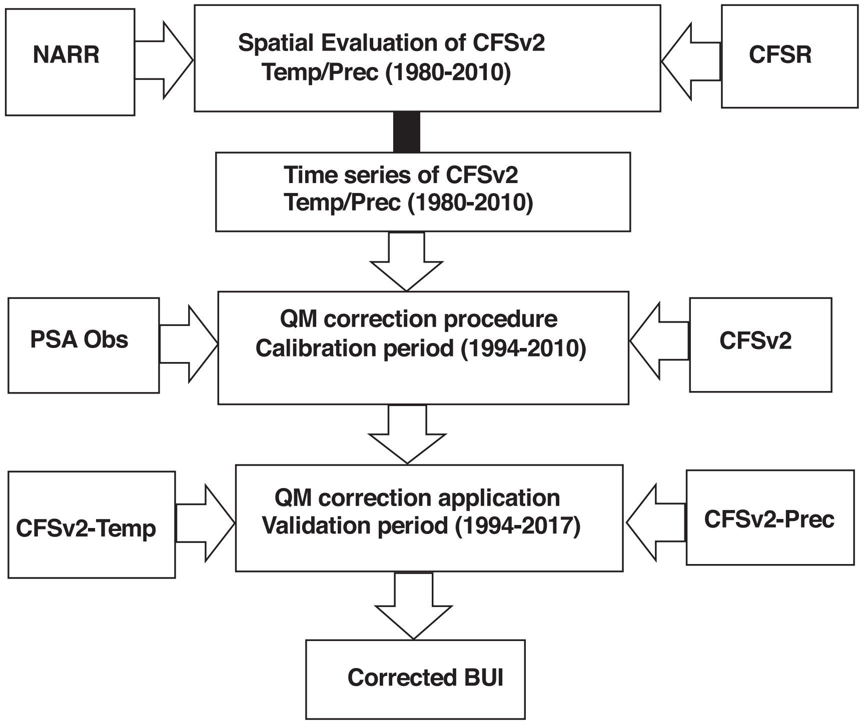

FIG. A1. The schematic view of the datasets analyzed in this study.

the observed BUI climatology over the PSAs. These results also suggest that additional postprocessing might shift the limits of predictability even further in detecting severe fire seasons.

The classification of corrected BUI ensemble members using quartiles reflects their usefulness for identifying severe fire events. The Q4 BUI forecasts tend to perform the best in predicting the observed BUI in the duff-driven season, while overestimating the BUI in the cumulative drought season. Moreover, the overestimates coincide with the severe fire events of 2004 and 2009 in the Tanana Valley West PSA (Fig. 12). This finding suggests that the usefulness of the CFSv2 ensemble forecasts with uncertainties can be tailored to user-specific needs by considering the observed patterns of boreal fires at the subseasonal to seasonal scale. Overall, this work demonstrates that the BUI values determined from the nonparametric QM-corrected forecasts can add value to firefighting preparation plans developed by fire managers when evaluating weather and fuel states in PSAs.

Furthermore, these findings illustrate the usefulness of CFSv2 seasonal forecasts from March for fire managers developing resource allocation plans for Interior Alaska. Therefore, to better serve the firefighting community, this study recommends a combination of gridded CFSv2 operational forecasts and the BUI system to produce operational BUI ensemble forecasts. The potential utility of the CFSv2 gridded forecasts for fire weather prediction in Interior Alaska is highlighted.

Acknowledgments. This work was supported by National Oceanic and Atmospheric Administration (NOAA) Climate Program Office's Modeling, Analysis, Predictions, and Projections Program, Grant NA16OAR4310142, by the National Science Foundation under Award OIA-1753748, and by the state of Alaska. The authors would like to express thanks to Randi Jandt for sharing her expertise on fire ecology and management. Similarly, the lead (corresponding) author would like to thank her advisor Prof. Nicole Mölders for mentoring and guidance in writing the paper, Profs. Kinchel Doerner and Javier Fochesatto for funding support, and Dr. Jamie L. Ward, as well as anonymous reviewers, for their helpful comments and discussions in shaping the paper into its final format. All datasets analyzed in this study have open access. Both the CFSv2 operational forecast and the CFSR monthly data can be retrieved from the NOAA data portal at https://www.ncdc.noaa.gov/data-access/model-data/modeldatasets/climate-forecast-system-version2-cfsv2. All Alaska fire history data has open access and can be obtained from this link http://forestry.alaska.gov/firestats/. The NARR data can be downloaded at ftp://ftp.cdc.noaa.gov/Datasets/NARR/.

APPENDIX

Data Analysis Overview

Figure A1 outlines the data processing steps carried out in this study.

REFERENCES

Arpaci, A., C. S. Eastaugh, and H. Vacik, 2013: Selecting the best performing fire weather indices for Austrian ecoregions. *Theor. Appl. Climatol.*, **114**, 393–406, https://doi.org/10.1007/s00704-013-0839-7.

Becker, E. J., and H. Van Den Dool, 2016: Probabilistic seasonal forecasts in the North American Multimodel Ensemble: A baseline skill assessment. *J. Climate*, **29**, 3015–3026, https://doi.org/10.1175/JCLI-D-14-00862.1.

——, E. H. Berbery, and R. W. Higgins, 2009: Understanding the characteristics of daily precipitation over the United States using the North American Regional Reanalysis. *J. Climate*, **22**, 6268–6286, https://doi.org/10.1175/2009JCLI2838.1.

——, H. Van Den Dool, and M. Peña, 2013: Short-term climate extremes: Prediction skill and predictability. *J. Climate*, **26**, 512–531, https://doi.org/10.1175/JCLI-D-12-00177.1.

Bond-Lamberty, B., S. D. Peckham, D. E. Ahl, and S. T. Gower, 2007: Fire as the dominant driver of central Canadian boreal forest carbon balance. *Nature*, **450**, 89–92, https://doi.org/10.1038/nature06272.

Bürger, G., J. Schulla, and A. T. Werner, 2011: Estimates of future flow, including extremes, of the Columbia River headwaters. *Water Resour. Res.*, **47**, W10520, https://doi.org/10.1029/2010WR009716.

Cannon, A. J., S. R. Sobie, and T. Q. Murdock, 2015: Bias correction of GCM precipitation by quantile mapping: How well do methods preserve changes in quantiles and extremes? *J. Climate*, **28**, 6938–6959, https://doi.org/10.1175/JCLI-D-14-00754.1.

Chapin, F. S., and Coauthors, 2008: Increasing wildfire in Alaska's boreal forest: Pathways to potential solutions of a wicked problem. *BioScience*, **58**, 531–540, https://doi.org/10.1641/B580609.

Dollard, J., 2020: Alaska Interagency Fire Danger Operating Plan. 75 pp., https://fire.ak.blm.gov/content/FuelFire/Alaska%20Fire%20Danger%20Operating%20Plan/Alaska%20FDOP%20Signed%202020-04-07.pdf.

Flannigan, M. D., M. A. Krawchuk, W. J. de Groot, B. M. Wotton, and L. M. Gowman, 2009: Implications of changing climate for global wildland fire. *Int. J. Wildland Fire*, **18**, 483, https://doi.org/10.1071/WF08187.

Freund, J. E., and B. M. Perles, 1987: A new look at quartiles of ungrouped data. *Amer. Stat.*, **41**, 200–203, https://doi.org/10.1080/00031305.1987.10475479.

Horel, J. D., and X. Dong, 2010: An evaluation of the distribution of remote automated weather stations (RAWS). *J. Appl. Meteor. Climatol.*, **49**, 1563–1578, https://doi.org/10.1175/2010JAMC2397.1.

——, R. Ziel, C. Galli, J. Pechmann, and X. Dong, 2014: An evaluation of fire danger and behaviour indices in the Great Lakes region calculated from station and gridded weather information. *Int. J. Wildland Fire*, **23**, 202, https://doi.org/10.1071/WF12186.

Hyndman, R. J., and Y. Fan, 1996: Sample quantiles in statistical packages. *Amer. Stat.*, **50**, 361–365, https://doi.org/10.2307/2684934.

Littell, J. S., D. McKenzie, D. L. Peterson, and A. L. Westerling, 2009: Climate and wildfire area burned in western U.S. ecoprovinces, 1916–2003. *Ecol. Appl.*, **19**, 1003–1021, https://doi.org/10.1890/07-1183.1.

McCorkle, T., J. Horel, A. Jacques, and T. Alcott, 2018: Evaluating the experimental High Resolution Rapid Refresh–Alaska modeling system using USArray pressure observations. *Wea. Forecasting*, **33**, 933–953, https://doi.org/10.1175/WAF-D-17-0155.1.

Mesinger, F., and Coauthors, 2006: North American Regional Reanalysis. *Bull. Amer. Meteor. Soc.*, **87**, 343–360, https://doi.org/10.1175/BAMS-87-3-343.

Mo, K. C., S. Shukla, D. P. Lettenmaier, and L.-C. Chen, 2012: Do Climate Forecast System (CFSv2) forecasts improve seasonal soil moisture prediction? *Geophys. Res. Lett.*, **39**, L23703, https://doi.org/10.1029/2012GL053598.

Nowacki, G. J., P. Spencer, M. Fleming, T. Brock, and T. Jorgenson, 2003: Unified ecoregions of Alaska: 2001. U.S. Geological Survey 02-297, https://doi.org/10.3133/ofr2002297.

Partain, J. L., and Coauthors, 2016: An assessment of the role of anthropogenic climate change in the Alaska fire season of 2015 [in "Explaining Extreme Events of 2015 from a Climate Perspective"]. *Bull. Amer. Meteor. Soc.*, **97** (12), S14–S18, https://doi.org/10.1175/BAMS-D-16-0149.1.

Pierce, D. W., D. R. Cayan, E. P. Maurer, J. T. Abatzoglou, and K. C. Hegewisch, 2015: Improved bias correction techniques for hydrological simulations of climate change. *J. Hydrometeor.*, **16**, 2421–2442, https://doi.org/10.1175/JHM-D-14-0236.1.

Rowe, J. S., and G. W. Scotter, 1973: Fire in the boreal forest. *Quat. Res.*, **3**, 444–464, https://digitalcommons.usu.edu/aspen_bib/5300.

Saha, S., and Coauthors, 2006: The NCEP Climate Forecast System. *J. Climate*, **19**, 3483–3517, https://doi.org/10.1175/JCLI3812.1.

——, and Coauthors, 2010: The NCEP Climate Forecast System Reanalysis. *Bull. Amer. Meteor. Soc.*, **91**, 1015–1058, https://doi.org/10.1175/2010BAMS3001.1.

——, and Coauthors, 2014: The NCEP Climate Forecast System version 2. *J. Climate*, **27**, 2185–2208, https://doi.org/10.1175/JCLI-D-12-00823.1.

Spillman, C. M., and O. Alves, 2009: Dynamical seasonal prediction of summer sea surface temperatures in the Great Barrier Reef. *Coral Reefs*, **28**, 197–206, https://doi.org/10.1007/s00338-008-0438-8.

Todd, S. K., and H. A. Jewkes, 2006: Wildland fire in Alaska: A history of organized fire suppression and management in the last frontier. Agricultural and Forestry Experiment Station Bull. 114, 65 pp., http://hdl.handle.net/11122/1313.

Van Wagner, C. E., 1987: Development and structure of the Canadian forest fire weather index system. Canadian Forest Service Tech. Rep. 35, 37 pp., http://cfs.nrcan.gc.ca/pubwarehouse/pdfs/19927.pdf.

Wang, Y., K. R. Anderson, and R. M. Suddaby, 2015: Updated source code for calculating fire danger indices in the Canadian Forest Fire Weather Index System. Canadian Forest Service, Northern Forestry Centre Information Rep. NOR-X-424, Natural Resources Canada, 26 pp., https://cfs.nrcan.gc.ca/publications?id=36461.

Wilks, D., 2006: *Statistical Methods in the Atmospheric Sciences*. 2nd ed. International Geophysics Series, Vol. 100, Academic Press, 648 pp.

——, and T. M. Hamill, 2007: Comparison of ensemble-MOS methods using GFS reforecasts. *Mon. Wea. Rev.*, **135**, 2379–2390, https://doi.org/10.1175/MWR3402.1.

Wood, A. W., L. R. Leung, V. Sridhar, and D. P. Lettenmaier, 2004: Hydrologic implications of dynamical and statistical approaches to downscaling climate model outputs. *Climatic Change*, **62**, 189–216, https://doi.org/10.1023/B:CLIM.0000013685.99609.9e.

Yuan, X., E. F. Wood, L. Luo, and M. Pan, 2011: A first look at Climate Forecast System version 2 (CFSv2) for hydrological seasonal prediction. *Geophys. Res. Lett.*, **38**, L13402, https://doi.org/10.1029/2011GL047792.

Zhao, T., J. C. Bennett, Q. J. Wang, A. Schepen, A. W. Wood, D. E. Robertson, and M.-H. Ramos, 2017: How suitable is quantile mapping for postprocessing GCM precipitation forecasts? *J. Climate*, **30**, 3185–3196, https://doi.org/10.1175/JCLI-D-16-0652.1.